CNRS
Centre National de la Recherche Scientifique

INFN
Istituto Nazionale di Fisica Nucleare

Advanced Virgo design: The Advanced LIGO approach for choosing modulation frequencies

VIR-066A-08

Stefan Hild, Maddalena Mantovani, Antonio Perreca and Andreas Freise

Issue: 1

Date: August 20, 2008

VIRGO * A joint CNRS-INFN Project
Via E. Amaldi, I-56021 S. Stefano a Macerata - Cascina (Pisa)
Secretariat: Telephone (39) 050 752 521 * FAX (39) 050 752 550 * Email W3@virgo.infn.it

Contents

1 Introduction

At the current stage of the design of the Advanced Virgo detector [3] many design options and parameters are not yet fixed. Decisions on parameters like the mirror curvature, modulation frequencies and design options such as the use of non-degenerate will have an high impact on the length sensing and control system. It is therefore at the moment impossible to define *the one* (optimal) length sensing and control system (LSCS). The development of the optimal LSCS will rather be a continuous evolution:

- taking into account and adopting to constraints given from other subsystems (for instance radii of curvature from OSD or potential tower positions from VAC)
- setting constraints and requirements for other subsystems (for instance the need for non-degenerate recycling cavities or reflectance of AR coatings in order to provide the actual necessary light power at the detection ports)

The consequence of the first item is that for every change of the detector design the LSCS has to be checked and if necessary be adjusted and reoptimised. The second item requires to find for each design option the best detector configuration in terms of LSCS and compare the achievable detector performance, in order to properly evaluate the consequences of each design option and providing input to the corresponding decision process.

As shown above it might be necessary to check, adjust or even completely redesign the Advanced Virgo LSCS several times within the next year. This means that all the usual calculations and simulations to determine the optimal detector configuration (for instance finding the optimal modulation frequencies and ensure their optimal resonance condition inside the various parts of the core interferometer) as well as evaluating the corresponding detector performance (for instance simulation of the optimised control matrix) need to be repeated over and over.

Therefore it seems to be highly beneficial to automate the process creating the optimal LSCS for advanced Virgo. In this document we present a set of tools, called **OSD_Tools** that can be used:

- to create the optimal detector configuration for a given set of input parameter and constraints.
- to evaluate the performance of such an optimal detector configuration (by calculating the best achievable controlability of the 5-DOF system).

Using the OSD-tools does not only provide automation to a certain extent, but also allows to ease up the documentation of the simulation itself.

1.1 Definition of Lengths

Figure 1 shows a simplified optical layout of the core optics of the Advanced Virgo interferometer. In the following we will distinguish between **distances**, **lengths** (indicated by a variable name starting with the letter 'L') and **tunings** (indicated by variables ϕ). We define a length as the distance between two objects measured to an accuracy of about 1 mm. The tuning (sometimes also refered to as microscopic distance) describes a sub-wavelength fraction of a distance. The actual distance between two objects can therefore be encoded by the length between the objects and the their tuning.

Name	Description
lprm	length between PRM HR coating and BS HR coating
lx	length between BS HR coating and IMX HR coating (includes BS and IMX substrates)
ly	length between BS HR coating and IMY HR coating (includes IMY substrate)
Lx	length between IMX HR coating and EMX HR coating
Ly	length between IMY HR coating and EMY HR coating
lsrm	length between BS HR coating and SRM HR coating (includes BS substrate)

Table 1: Definition of the lengths inside the Advanced Virgo core interferometer.

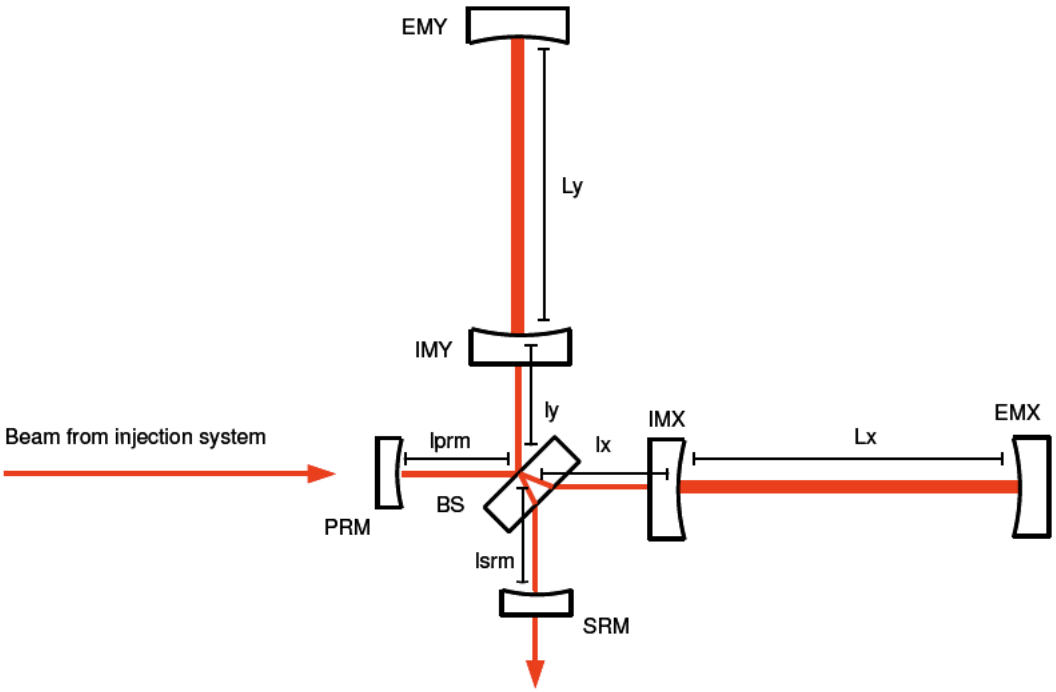

Figure 1: Simplified schematic of the Advanced Virgo optical layout (from [1]). The Power-Recycling mirror (PRM), the beam splitter (BS) and the Signal-Recycling mirror (SRM) form together with the 4 mirrors (IM = input mirror, EM = end mirror) of the two arm cavities (X-arm and Y-arm) the core optics of Advanced Virgo. A detailed description of the used lengths and degrees of freedom is given in the text.

Table 1 gives a description how exactly the lengths are defined. Please note that some lengths might consist of several paths and also include path length inside mirror substrates. A few lengths which are of special interest from LSCS point of view are described in more detail in the following subsections.

1.1.1 Schnupp length

The Schnupp length, L_{Sch}, or Schnupp asymmetry is necessary to allow the detection of radio frequency modulation sidebands at the output port of the interferometer. By making lx and ly of a different macroscopic length we can ensure the radio frequency modulation sidebands to be transmitted to the antisymmetric port. We define the Schnupp length to be:

$$L_{\mathrm{Sch}} = \frac{\mathrm{lx} - \mathrm{ly}}{2}. \tag{1}$$

1.1.2 Length of the Power-Recycling cavity

For the macroscopic length of the Power-Recycling cavity (PRC) we will use the following definition:

$$L_{\mathrm{PRC}} = \mathrm{lprm} + \frac{\mathrm{lx} + \mathrm{ly}}{2}. \tag{2}$$

1.1.3 Length of the Signal-Recycling cavity

Analogous we can define the macroscopic length of the Signal-Recycling cavity (SRC) to be:

$$L_{\mathrm{SRC}} = \mathrm{lsrm} + \frac{\mathrm{lx} + \mathrm{ly}}{2}. \tag{3}$$

1.2 Definition of Degrees of Freedom (DFO)

The main purpose of a LSCS is to keep all core mirrors at their operation points. We can use the following five degrees of freedom to describe the full core interferometer:

$$\phi_{\mathrm{DARM}} = \frac{\mathrm{Lx} - \mathrm{Ly}}{2} \mod \lambda \tag{4}$$

$$\phi_{\mathrm{CARM}} = \frac{\mathrm{Lx} + \mathrm{Ly}}{2} \mod \lambda \tag{5}$$

$$\phi_{\mathrm{MICH}} = \frac{\mathrm{lx} - \mathrm{ly}}{2} \mod \lambda \tag{6}$$

$$\phi_{\mathrm{PRCL}} = \mathrm{lprm} + \frac{\mathrm{lx} + \mathrm{ly}}{2} \mod \lambda \tag{7}$$

$$\phi_{\mathrm{SRCL}} = \mathrm{lsrm} + \frac{\mathrm{lx} + \mathrm{ly}}{2} \mod \lambda \tag{8}$$

The first 4 degrees of freedom are identical to the standard ones present in initial Virgo. Please note that the above defined 5 degrees of freedom correspond to microscopic mirror positions.

1.2.1 Dark fringe offset (dfo)

In order to realize DC-readout for Advanced Virgo it is necessary to introduce a dark fringe offset (dfo) which will be used to transmit a small amount of TEM_{00} carrier light to the output port, where it is used as local oscillator (LO). Please note that the dark fringe offset is a microscopic position, i.e a tuning, which is defined as the DC part of the DARM degree of freedom:

$$\phi_{\mathrm{dfo}} = \phi_{\mathrm{DARM}}(0\,\mathrm{Hz}) = \frac{\mathrm{Lx} - \mathrm{Ly}}{2} \mod \lambda \tag{9}$$

1.3 Automation LSCS simulations: OSD_Tools

Within the context of the Advanced Virgo subsystem for Optical Simulation and Design (OSD) [5] we have developed the **OSD-Tools package**, a collection of Matlab functions for optical design tasks. The OSD-Tools make use the numerical interferometer simulation software **Finesse** [4] (available at `http://www.rzg.mpg.de/~adf/`)[1]. All relevant scripts and files are stored in a subversion repository which provides backup as well as version control. This svn repository is accessible to everyone without username and password (server: `svn://lnx0.sr.bham.ac.uk`, repository: `adv-osd`).

1.4 Optimisation order

Our optimisation of the detector configuration is based on the "AdvLIGO Interferometer Sensing and Control Conceptual Design" (LIGO-T070247-01-I) [2].

[1] However, the OSD-Tools do not rely on the use of Finesse. With small effort it is possible to adapt all OSD-Tool functions to work with other simulations tools, such as for instance Optickle.

Since many of the detector parameters that need to be optimized, depend on other detector parameters, there is a natural order in which the optimization has to be performed. The main detector parameters are determined in the following order:

1. Radii of curvature of the mirrors
2. RF-modulation frequencies
3. Length of Power-Recycling cavity (PRC)
4. Schnupp Asymmetry
5. Length of Signal-Recycling cavity (SRC)

After this optimization we are able to simulate for this detector configuration the control matrix, which can then be fine-tuned by another optimization round including the following steps:

- Choice of the dark fringe offset (dfo)
- Choice of demodulation phases
- Choice of photo diodes actually used
- Choice of modulation indices
- Choice of the reflectance of the AR coatings to give the required optical power at the corresponding detection ports.

In the following Sections we describe step by step how the optimization of the main detector parameters is done.

2 Calculating the test mass curvature for a given beam size

Figure 2 illustrates the dependence of the test mass ROC on the beam size for a symmetric cavity of 3 km length. The first optimization steps calculates the mirror radii of curvature (ROC) for a desired beam radius ($1/e^{-2}$ in power). The Matlab function **OSD_ROC.m** executes FINESSE simulations in order to determine the ROC of the main arm cavity mirrors (IMx, EMx, IMy, EMy) and the two recycling mirrors (PRM and SRM).

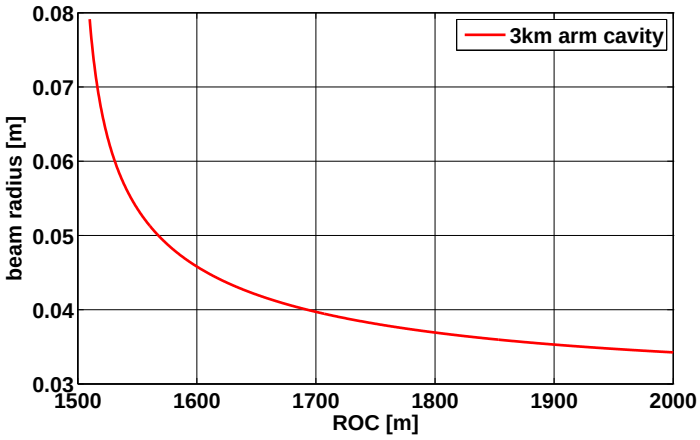

Figure 2: Beam radius ($1/e^{-2}$ in power) versus mirror radius of curvature (ROC) for a symmetric cavity of 3 km length.

In a first simulation step the beam size of the cavity eigenmode is simulated for a scan (from $\frac{L}{2}+1$ to $L-1$) of the ROC of the main cavity mirrors. The beam radius at the main test masses is extracted by using the

FINESSE beam parameter detector. In order to determine the ROC of PRM and SRM a second FINESSE simulation is performed. Using beam parameter detectors at the position of the high reflectance (HR) coatings we can simulate the exact beam parameters at the position of the recycling mirrors, taking into account all optics between the arm cavities and the recycling mirrors, such as input mirror substrates (concave lens), the beam splitter (including potential thermal lensing) or potential compensation plates. Using the distance from the waist, z, and the Rayleigh range, z_r we can calculate the wavefront curvature at the position of the recycling mirrors, i:

$$R_{c,i} = z_i + \frac{z_{r,i}^2}{z_i}; \tag{10}$$

The corresponding optimized values for the ROC of PRM and SRM as well as for the main cavity mirrors are finally written into the Finesse output file and also displayed on the screen. Also the waist size (in the center of the arm cavity) is calculated and displayed on the screen.

3 Choosing optimal RF modulation frequencies

This function calculates the optimal values for two radio frequency (RF) modulations. The main constraint for this choice is that both modulation frequencies should simultaneously be resonant inside the PRC. This can be realized making both frequencies harmonics of the free spectral range (FSR) of the PRC. If we choose the first modulation frequency, f_1, to be at the first FSR then, we have to choose the second modulation frequency, f_2, to be a multiple of the first modulation frequency

$$f_2 = M \cdot f_1 \qquad \text{with} \quad M \in \mathbb{N}. \tag{11}$$

The best choice of M needs to be determined in a trade-off process of best decoupling of f_1 and f_2 (want to make M as large as possible) and the feasibility of f_2 (want to make M as small as possible to allow for simpler RF electronics and larger photo diodes).

In order to decouple the various length degrees of freedom as much as possible both pairs of sidebands from the two RF modulation should not be resonant inside the arm cavities. Furthermore (similar to the Advanced LIGO approach [2]), not only the fundamental optical mode (TEM_{00}) of the modulation sidebands are not allowed to be resonant inside the arms, but also the first six higher order modes (TEM_{lm} with $l + m \leq 6$) have to be off resonance.

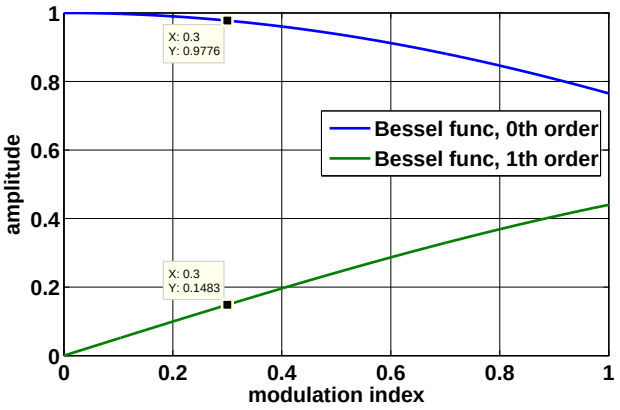

Figure 3: Fundamental and 1st order Bessel functions. For large modulation indices the amplitude of the 1st order Bessel function starts to significantly contribute. For instance with using an modulation index as large as 0.3 will yield that more than 10 % of the modulation is present at twice the modulation frequency.

Due to the fact that we might have to use rather large modulation indices (such as 0.3) we will in addition demand that also the first harmonic of the modulation frequencies ($2 \cdot f_1$ and $2 \cdot f_2$) and their first six higher order optical modes have to be off resonant inside the arm cavities. This condition is equivalent to f_1 and f_2 (and their first six higher order optical modes) not being exactly at the anti-resonance of the arm cavity.

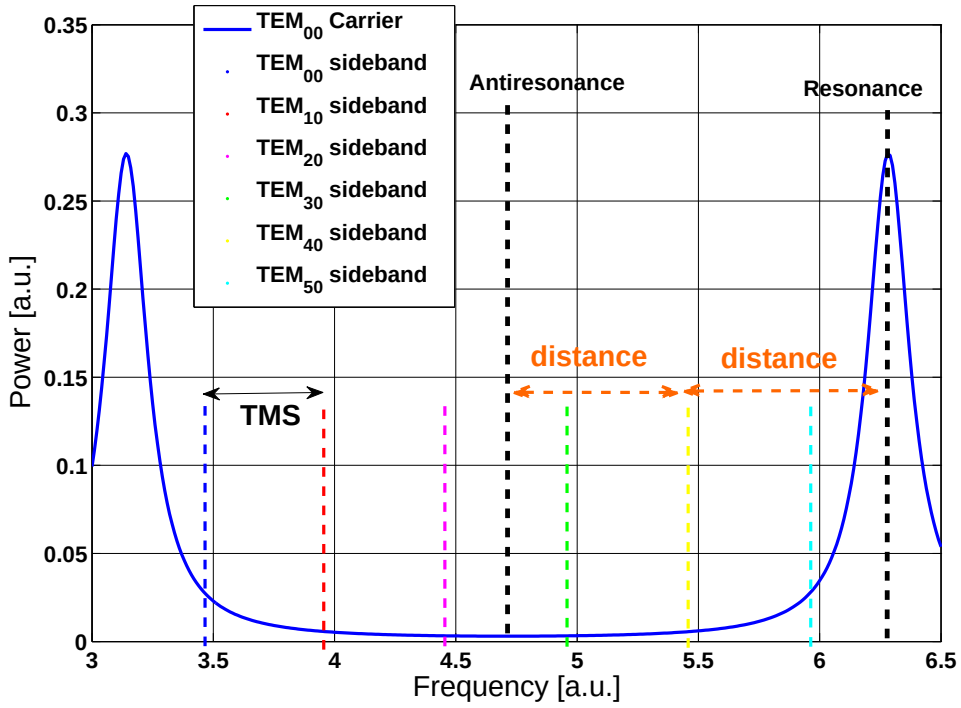

Figure 4: Schematic illustration of the resonance condition of the modulation sidebands inside the arm cavities. A detailed explanation can be found in the text.

In order to fulfill as well as possible the conditions stated above we calculate the frequency of all four modulation sidebands ($+f_1$, $-f_1$, $+f_2$ and $-f_2$) and their first six higher order optical modes, all together 28 frequencies. The frequency $f_{i,l+m}$ of the TEM_{lm} of the modulation sideband f_i can be computed as

$$f_{i,l+m} = f_i + f_{\mathrm{sep},l+m}, \tag{12}$$

where $f_{\mathrm{sep},l+m}$ is the transversal mode spacing of the optical mode of the order $l+m$, which can be computed as follows:

$$f_{\mathrm{sep},l+m} = (l+m) \times \frac{c}{2\pi L} \arccos \sqrt{(1-\frac{L}{R_{c,i}})(1-\frac{L}{R_{c,e}})}, \tag{13}$$

with L being the length of the arm cavity and $R_{c,i}$ and $R_{c,e}$ being the radius of curvature of the input mirrors and the end mirrors, respectively. In the next step we find the distance $\Delta_{i,l+m}$ of these 28 frequencies from the resonance of the arm cavity:

$$\Delta_{i,l+m}(f) = k \cdot \mathrm{FSR} - f_{i,l,m}(f), \tag{14}$$

where $FSR = c/(2 \cdot L)$ is the free spectral range of the arm cavities and k is an integer number describing the free spectral range closest to $f_{i,l+m}$. Analogous to the 28 distances $\Delta_{i,l+m}$ we can calculate the 28 values $\Gamma_{i,l+m}$, describing the distance of the modulation sidebands from anti-resonance:

$$\Gamma_{i,l+m}(f) = (k+\frac{1}{2}) \cdot \mathrm{FSR} - f_{i,l+m}(f), \tag{15}$$

Figure 4 shows an illustrating sketch of the resonance condition of the modulation sidebands inside arm cavity. The two blue peaks indicate the resonances inside the arm cavities, separated by one FSR. One modulation sideband and its higher order modes are denoted by the comb of equally separated vertical dashed lines. For the 4th higher order optical mode (yellow dashed line) distance to resonance and anti-resonance is indicated by the two orange dashed arrows.

Finally we take the minimal distance ($\Lambda(f)$) out of the 56 distance values (28 from $\Delta_{i,l+m}(f)$ and 28 from $\Gamma_{i,l+m}(f)$) and use this value as a figure of merit for the choice of the modulation frequencies. All these calculations are performed by the OSD-Tool function **OSD_modfreq.m** and its subroutines OSD_mode_spacing.m, OSD_mode_spacing_plot_dist.m, OSD_mode_spacing_plot_freq.m, OSD_save_plot.m, OSD_savematrix.m and OSD_plotall.m. The functions scans the modulation frequencies over a given frequency range, choose the one providing the largest value of $\Lambda(f)$ and writes the optimized modulation frequencies in the Finesse output file and also displays them on the screen. In addition some auxiliary plots and a tabular containing all values of $\Delta_{i,l+m}(f)$ and $\Gamma_{i,l+m}(f)$ are produced in the background and saved to subdirectories.

4 Choosing the length of the Power-Recycling cavity (PRC)

The main constraint for the length of the PRC is to have both modulation frequencies, f_1 and f_2, being resonant in the PRC. We define the length of the PRC as a the single trip optical path-length between the HR coating of the Power-Recycling mirror (PRM) and the averaged distance to the HR-coatings of the input test masses. The resonance condition can be expressed by the following equation:

$$L_{\mathrm{PRC}} = (N + 0.5)\frac{c}{2f_1}. \tag{16}$$

Due to the fact that f_2 was previously chosen to be the M-th harmonic of f_1, f_2 will always be resonant as long as f_1 is resonant in the PRC.

Choosing the length of the PRC is done by OSD-Tool function **OSD_PRC_length.m**. As an input to this function one has to give the desired rough length of the PRC (for example about 10 m for the current optical layout, but you can also give in 100 m if you want to have a long non-degenerate PRC). The function then automatically determines the best value for N (see Equation 16) and finally writes the new length to lprm. In a last step a Finesse simulation is carried out (similar to the one described in Section 2) to find the optimal ROC of PRM for the new length of the PRC.

5 Choosing the Schnupp asymmetry and the length of the Signal-Recycling cavity (SRC)

In order to provide maximum decoupling of the SRCL from all other degrees of freedom we want only the f_2 modulation sidebands to be resonant in the SRC, i.e. the f_1 sidebands should be explicitly off resonant in the SRC. Hence we have to choose the Schnupp asymmetry and the SRC in a way to maximize the f_2 signals while keeping the f_1 signals as low as possible.

Figure 5 shows the power of the RF modulation sidebands, f_1 (lower subplot) and f_2 (upper subplot), inside the SRC for a simultaneous scan of L_{Sch} and L_{SRC}. As one can see the power of the f_2 sideband shows two distinct maxima for different Schnupp lengths. The first maximum, referred to as short Schnupp length option, appears at about $L_{\mathrm{Sch}} = 0.05\,\mathrm{m}$, while a second maximum appears for a Schnupp length of about half a meter. The latter one will be referred to as long Schnupp length option.

After choosing the optimal Schnupp length, in a second step the optimal SRC length needs to be chosen. As show in Figure 5 the optimal SRC length depends on the choice of the Schnupp length (short or long option).

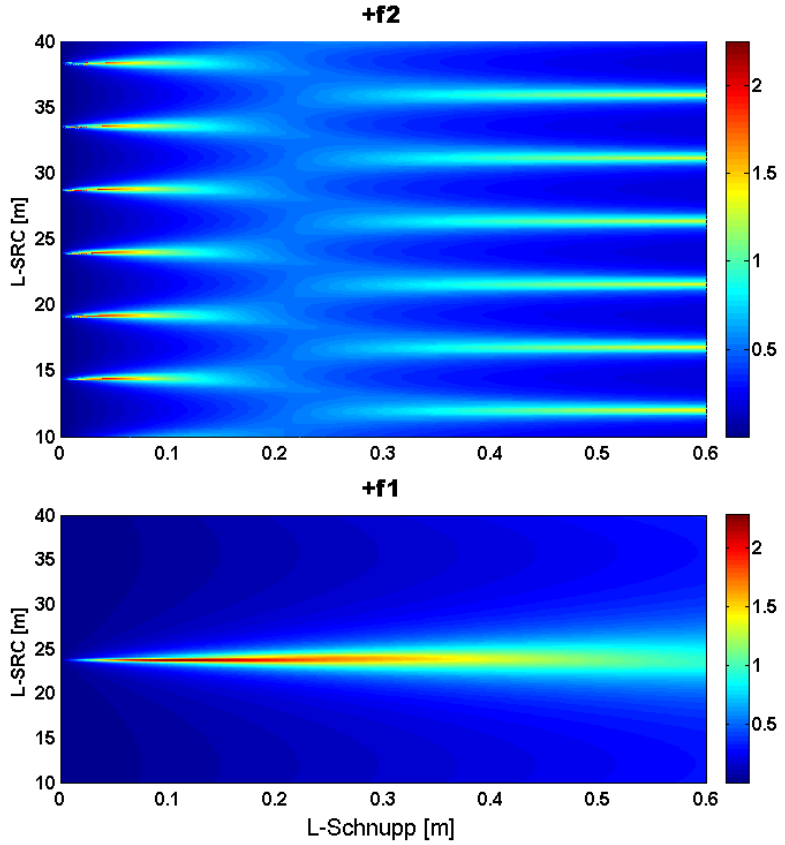

Figure 5: Plot of the optical power of the two RF modulation sidebands, f_2 (upper subplot) and f_1 (lower subplot), inside the SRC. The scan is over the Schnupp length L_{Sch} (x-Axis) and the length of the SRC L_{Sch} (y-Axis). The power of the f_2 sideband gets maximal for two different Schnupp lengths: One maximum is obtained for very small Schnupp lengths (about 0.05) and the second maximum can be achieved with a rather long Schnupp length (about 0.6). From the upper plot it can also be seen that the optimal length of the SRC depends on whether the short or long Schnupp length option is chosen. In order to get good decoupling of the different DFO of the LSCS we want f_1 to be off resonance in the SRC cavity, i.e. we must not choose L_{SRC} to be about 24 m.

Both the optimal L_{Sch} and L_{SRC} are chosen simultaneously by the same OSD-Tool function called **OSD_SR_Schnupp.m**. As input arguments this function needs to get the Schnupp length option (0 = short, 1 = long) and a rough length of the desired SRC length. The function finds the optimal set of L_{Sch} and L_{SRC} to maximize the f_2 power inside the SRC and afterwards recalculates the ROC of SRM to adopt for the changed length of the SRC. Please note that OSD_SR_Schnupp.m does not automatically take the strength of the f_1 sideband inside the SRC into account.

6 Example of an OSD routine for basic optimisation of the Advanced Virgo detector configuration

The OSD-tool functions described in the Sections 2 to 5 are able to automatically perform the full detector optimisation described in the enumeration of Section 1.4 (mirror ROCs, modulation frequencies, length of PRC, SRC and Schnupp asymmetry) starting from a Finesse parameter file as input.

```
%-------------------------------------------------------------------------
% Script to optimize the Advanced Virgo detector configuration.
%
% Starting from the actual AdV base file, this script optimizes:
%  1. the mirror ROCs for a given beam size
%  2. the two modulation frequenies
%  3. the PRC length
%  4. the Schnupp length
%  5. the SRC length
%
% The optimised parameters and lengthes are displayed on
% the screen and also written into a new Finesse input file
% called: "optimized_detector_25072008.kat"
%
% Stefan Hild 14.07.2008 hild@star.sr.bham.ac.uk
%-------------------------------------------------------------------------

% Starting from the actual base file we calculate new
% mirror ROCs for the wanted beam size of 55cm.
OSD_ROC(0.055, 'advirgo_base_08072008', 'test_25072008')

% Optimising modulation frequencies
% Scanning plus minus 30kHz around 6.246MHz using 20 Hz step size.
% f2 is chosen to be 5 times f1.
OSD_modfreq('test_25072008', 'test_25072008a', 6.246e6, 3e4, 20, 5)

% Optimising the PRC-length. Rough length of PRC should be about 10m.
OSD_PRC_length(10, 'test_25072008a', 'test_25072008b')

% Optimising the SRC-length and the Schnupp-length.
% 0 means that we go for short Schnupp length option.
% The rough length of the SRC shall be about 15m.
OSD_SR_schnupp('test_25072008b', 'optimized_detector_25072008', 15, 0)
```

Figure 6: Screen-shot of example script showing how easy the optimization of the Advanced Virgo detector configuration is using the OSD-tools. This script queries consecutively the four top-level OSD-tool functions `OSD_ROC.m`, `OSD_modfreq.m`, `OSD_PRC_length.m` and `OSD_SR_Schnupp.m`. The optimized parameter file produced by each function is used as input file of the proximate function.

In a very easy way a series of OSD-tool functions can be used to do the full optimisation process. Each of the OSD-tool functions displays the optimised parameters on the screen and in addition also writes them into an optimized Finesse parameter file. As shown in Figure 8 we can now combine several OSD-tool functions in a way: The optimised parameter set of one function is used as input parameter set of the next function. Finally the output file ('optimized_detector_25072008.kat') of the last function ('OSD_SR_Schnupp.m') contains an optimized Advanced Virgo configuration.

7 Appendix A: Computing the control matrix and choosing the best photodiodes

7.1 Computing the full control matrix

In order to evaluate the performance of one LSCS configuration and compare it to a different one, it is necessary to compute the full longitudinal control matrix of both systems and compare their controlability. Figure 7 shows schematically the potential 7 control ports of Advanced Virgo. The following abbreviations have been used: SP: symmetric port, AP: antisymmetric port, POBS: pick-off beam splitter AR, POX: pick-off input mirror X-arm AR, POY: pick-off input mirror Y-arm AR, XP: X-arm transmission and YP: Y-arm transmission.

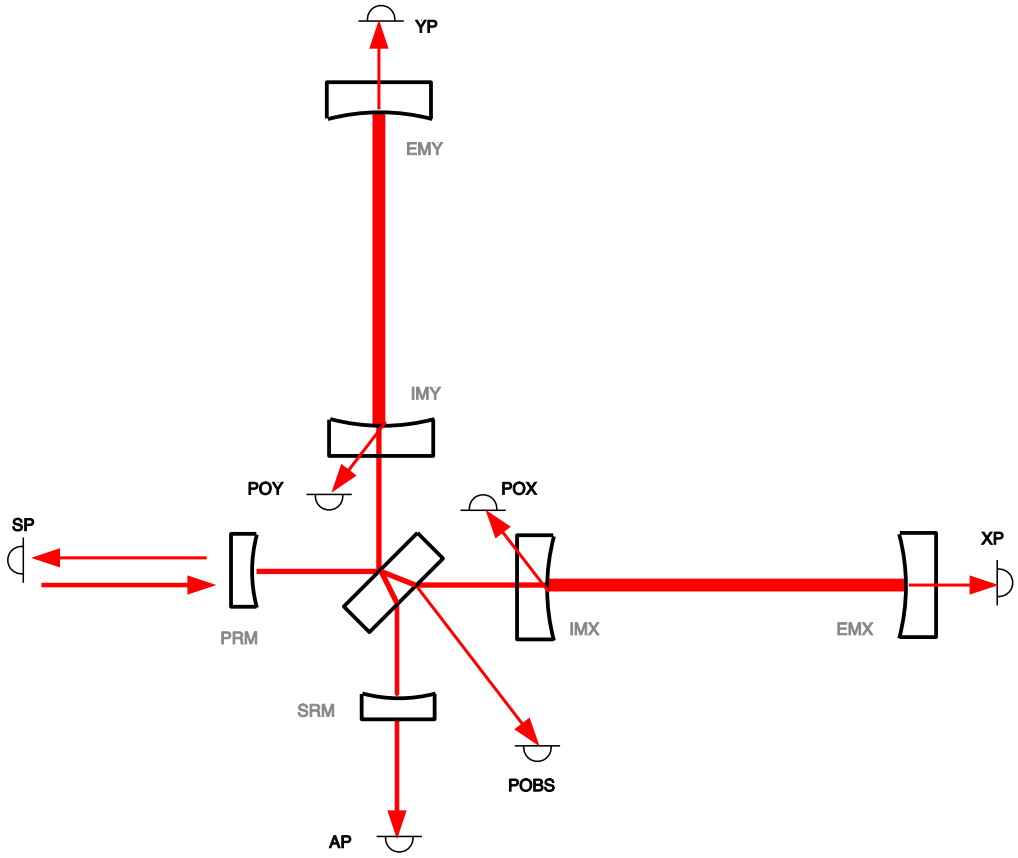

Figure 7: Sketch of the Advanced Virgo optical layout defining the names of the detection ports (from [1]). The abbreviations are explained in the text.

At all of these 7 detection ports we can position various photodiodes that look at all interesting light fields. At each detection port we use the following 5 photo diode types:

- demodulated at f_1, demodulation phase 0 deg.
- demodulated at f_1, demodulation phase 90 deg.
- demodulated at f_2, demodulation phase 0 deg.
- demodulated at f_2, demodulation phase 90 deg.
- DC detection (not demodulated)

Since we do not know at this stage of the analysis which photo diode type at which detection port will give the best signal for a certain degree of freedom, we do not restrict ourselves, by excluding any photo diode from the control matrix. Thus we get a control matrix with 5 columns (degrees of freedom) and 35 rows (photodiodes).

The OSD-tool function computing the full control matrix using FINESSE [2] is called `OSD_fullcontrolmatrix.m`.

7.2 Finding the 5 best photodiodes

In the next step we want to reduce the 5×35 control matrix to a quadratic 5×5 matrix using the five best photo diode signals available from the full control matrix. This can be done using the OSD-tool function `OSD_submatrix`, which evaluates for each possible 5-diode subset (of the full control matrix) the achievable controlability. Following Chapter 6 of [6] this function uses the *minimum separation angle computed with the submatrix* and the *volume spawn by the submatrix* as figure of merit for the controlability.

Our function also allows the possibility to apply hierarchical control in order to further improve the controlability of the system, further decoupling the system.

8 Appendix B: How to go on from here? Fine tuning of the control matrix

In this section we describe briefly the steps that are likely to be necessary for the transition from a *preliminary LSCS* to a *mature LSCS*. These steps are far beyond the scope of this document and shall therefore just be mentioned here:

1. Choice of demodulation phases
2. Choice of the dark fringe offset (dfo)
3. Choice of modulation indices
4. Choice of the reflectance of the AR coatings to give the required optical power at the corresponding detection ports.

8.1 Choice of demodulation phases

The choice of the proper demodulation phases for the used photo diodes is crucial to achieve a well controllable and low noise system. Especially for detuned Signal-Recycling it cannot be expected to find the best signals for demodulation phases exactly at 0 and 90 degree [7].

The OSD-tool function `OSD_optimization.m` can perform the simultaneous optimization of the several photo-diodes. It scans the demodulation phase of one or more photo detectors and computes for all combinations the maximum controlability of the system. Please note that this optimisation routine is computational as well as time intensive (but can be improved by only optimising a subset of photo diodes).

8.2 Choice of the dark fringe offset

The choice of the optimal dark fringe offset is at this stage of the Advanced Virgo design not possible. The optimal choice of this key parameter depends on so many other parameters which are not fixed or not known at the moment, that it is impossible to do any optimisation.

[2] Please note that FINESSE is not the optimal software to compute the control matrix of any high power configuration of Advanced Virgo. This is due to the fact that FINESSE does not take radiation pressure into account.

With a lot of simplification it can be said that the optimal dark fringe offset needs to be decided by a trade off of the coupling of technical noise sources (the larger the dfo the larger the noise coupling) and composition of the output port light field (the more higher order light is present the larger the dfo needs to be).

8.3 Choice of modulation indices and reflectivities of AR coatings

The choice of the modulation indicies and the reflectivities of the AR coatings for the pick-off ports are connected. In order to not spoil the Advanced Virgo sensitivity by introducing control noise, we have to ensure that the photo diode signals used for the LSCS provide a sufficient signal to shot noise ratio. In general the signal to shot noise ratio at the photo diodes can be increased by increasing the light power (increase of AR coating reflectivity) and/or by increasing the corresponding modulation index (of course this option only works for demodulated signals).

9 Appendix C: Flow diagram of the basic OSD-tool functions

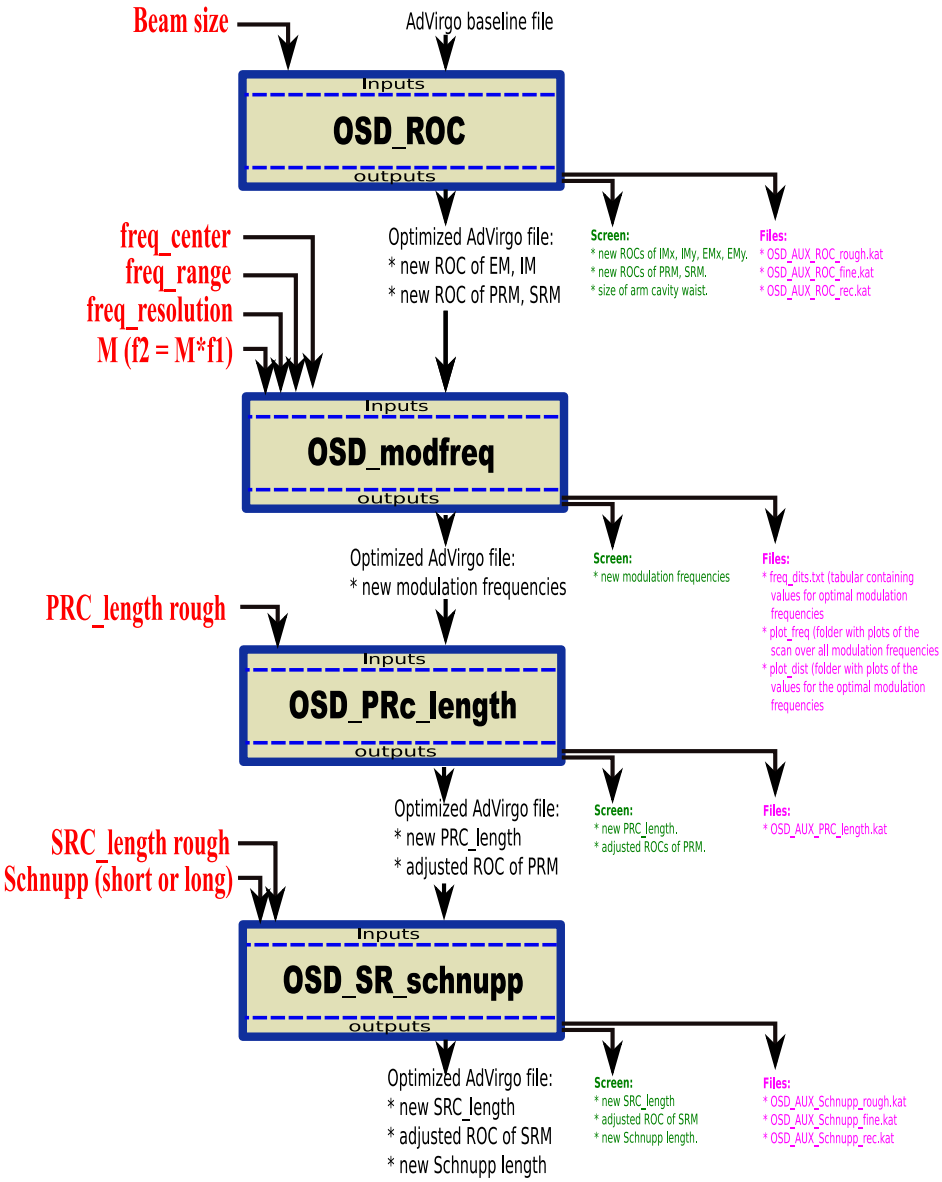

Figure 8: Flow diagram of the OSD-tools functions used for the basic optimisation of the Advanced Virgo detector configuration.

References

[1] M. Mantovani, A. Freise, "Initial set of optical parameters for numerical simulations towards Advanced Virgo" Virgo note VIR-002B-07 3, 11

[2] Rich Abbott, Rana Adhikari, Stefan Ballmer, Lisa Barsotti, Matt Evans, Peter Fritschel, Valera Frolov, Guido Mueller, Bram Slagmolen, Sam Waldman: "AdvLIGO Interferometer Sensing and Control Conceptual Design", Technical Note, LIGO-T070247-01-I, 2008/04/08 4, 6

[3] The Advanced Virgo Team, "Advanced Virgo Conceptual Design", Virgo note VIR-042A-07 2

[4] A. Freise, G, Heinzel, H. Lück, R. Schilling, B. Willke and K. Danzmann: 'Frequency-domain interferometer simulation with higher-order spatial modes', Class. Quantum Grav. **21** (2003)1067–1074. 4

[5] The Advanced Virgo OSD wiki can be accessed via the Advanced Virgo web page (http://wwwcascina.virgo.infn.it/advirgo/). Please use the link to the 'Adv Wiki' and then proceed to the 'OSD Wiki'. 4

[6] M. Mantovani "The Automatic Alignment in the Virgo interferometer", PhD Thesis (2007) 12

[7] S. Hild et al "Demonstration and comparison of tuned and detuned signal recycling in a large-scale gravitational wave detector" *Classical and Quantum Gravity* **24** (2007) 1513-1523 12